# RESEARCH ARTICLE

# Application of DTI and ARFI imaging in differential diagnosis of parotid tumours

[1,2]Jinfen Yu, [3]Yanfei Du, [2]Yong Lu, [4]Weidong Zhang, [4]Dongsheng Zhang, [1]Guangbin Wang and [1]Chuanting Li

[1]Shandong Medical Imaging Research Institute, Shandong University, Jinan, Shandong, China; [2]Traditional Chinese Medical Hospital, Zhangqiu, Shandong, China; [3]Liaocheng People's Hospital, Liaocheng, Shandong, China; [4]Shandong Provincial Hospital, Shandong University, Jinan, Shandong, China

**Objectives:** To explore the utility of diffusion tensor imaging (DTI) and acoustic radiation force impulse (ARFI) imaging in the diagnosis of parotid tumours.
**Methods:** 51 patients with parotid tumours were examined with DTI on 3.0-T MRI and ARFI imaging on an ultrasound scanner before surgery. Values of apparent diffusion coefficient (ADC), fractional anisotropy (FA) and shear-wave velocity (SWV) were calculated and analyzed with independent samples Wilcoxon–Mann–Whitney test. Cut-off values, sensitivity and specificity were calculated with receiver-operating characteristic (ROC) curve analysis. The value of combination was calculated through parallel test for the cut-off value of ADC, FA and SWV (combination = 0 or 1); then, ROC analysis was performed with pathological results as the gold standard to calculate the sensitivity and specificity for the combination of the three parameters distinguishing benign and malignant parotid tumours. Pathological diagnosis for every patient was made post-operatively from the tumour tissue taken during operation.
**Results:** There was a significant difference between benign and malignant tumours in the values of ADC, FA and SWV ($p = 0.032$, $p = 0.011$ and $p < 0.0001$); a significant difference in the values was also found between pleomorphic adenoma and malignant tumour ($p = 0.0012$, $p < 0.0001$ and $p = 0.0002$). The diagnosis cut-off points between benign and malignant tumours for ADC, FA and SWV were $1.02 \times 10^{-3}$ mm$^2$ s$^{-1}$, 0.24 and 2.76 m s$^{-1}$, respectively; the sensitivity for ADC, FA and SWV was 87.50, 62.50 and 68.75%; the specificity was 45.71, 82.86 and 97.14%. Analysis of the combination of the three parameters increased the sensitivity, specificity, Youden index and area under the ROC curve compared with analysis of each parameter alone for distinguishing benign and malignant tumours.
**Conclusions:** The diagnostic value of the combination of the three parameters for distinguishing benign and malignant parotid tumours is the best; SWV is the preferred indicator. Parameters of DTI and ARFI may reflect the histological characteristics of parotid tumours and predict benignancy and malignancy and could provide quantitative information about the tumour. Combination of DTI with ARFI imaging had obvious advantage for the diagnosis of parotid tumours than each alone.
*Dentomaxillofacial Radiology* (2016) **45**, 20160100. doi: 10.1259/dmfr.20160100

**Cite this article as:** Yu J, Du Y, Lu Y, Zhang W, Zhang D, Wang G, et al. Application of DTI and ARFI imaging in differential diagnosis of parotid tumours. *Dentomaxillofac Radiol* 2016; **45**: 20160100.

## Introduction

Parotid tumours account for approximately 3% of all head and neck tumours.[1] Parotid glands exhibit the largest variety of histologic types and subtypes of primary neoplasms, except female genital system neoplasms.[2] 80% of parotid tumours are benign tumours, with about 85% of benign tumours being pleomorphic adenoma. Surgery is the most effective approach for parotid tumour management,[3] and pre-operative histological diagnosis as well as qualitative evaluation of tumour histological properties before surgery is crucial. Tumour resection of pleomorphic adenoma without histological confirmation before surgery would result in 20–45% of risk of local recurrence;[4–7] it would be reduced to about 1.5–6% by excision of the lateral parotid gland with facial nerve preservation.[3,8,9] Moreover, the risk of facial paralysis and malignant transformation would be increased by repeated operations.[10]

Ultrasound, MRI and CT are non-invasive approaches and are commonly used for the evaluation of parotid lesions. However, these conventional imaging approaches are less precise owing to the overlap in the appearance of parotid tumours.[11–14]

Diffusion-weighted imaging is a technique that could obtain the spatial diffusion map of free-water protons for evaluating molecular diffusivity under motion restriction within the tissues and could be measured with the apparent diffusion coefficient (ADC).[15] Diffusion tensor imaging (DTI) is an extension of diffusion-weighted imaging and could measure the incoherent directional distribution of diffusivity with fractional anisotropy (FA).[16,17] The FA or ADC value has a strong correlation with cell density,[18] and malignant tumours usually have a reduced ADC value and an elevated FA value.[19,20] While DTI is widely applied in multiple organs,[18,21–24] its application, particularly the FA value in parotid tumours, is rarely reported.

Acoustic radiation force impulse imaging (ARFI) describes mechanical tissue properties.[25] Briefly, the application of acoustic push pulses generates localized displacements within a selected region, whose shear-wave velocities (SWVs) can be measured by ultrasound waves and expressed quantitatively in metre per second. SWV has a positive correlation with tissue elasticity and hardness. The stiffer the tissue, the higher the SWV will be. It could quantitatively measure the elasticity properties and assess the tissue structure changes and tissue stiffness of tumours.[25] Stiffness of tumours could be changed with alterations of cancer cellular density and components of the tissue and blood vessels. The application of SWV in the diagnosis of parotid tumour has been reported by several studies.[25,26] SWV might effectively differentiate benign from malignant tumours, pleomorphic adenoma from adenolymphoma.

Our study aimed to determine the feasibility of ADC, FA and SWV for the differential diagnosis of parotid tumours. The utility value of these three parameters' combination was also explored.

## Methods and materials

### Subjects

51 patients with histopathologically diagnosed parotid tumour post-operation were included in this study (18 males and 15 females); the mean age was 45 years (range 6–71 years). The course of disease was from 3 months to 10 years. Two doctors (with 25 and 28 years' experience in oral maxillofacial surgery and pathology) reviewed the operation and biopsy results. Consensus was reached in between the two reviewers in relation to the histopathological diagnosis. In cases of disagreement, a third reviewer (a radiologist and pathologist with 28 years' experience) was consulted for a settlement. The inclusion criteria were as follows: (1) patients who were histopathologically diagnosed post-operation based on classification of head and neck tumours in World Health Organization 2005;[27] (2) patients without any invasive examinations and any treatments including biopsy, radiation and chemotherapy before MRI and ARFI inspection; and (3) patients with high-quality diffusion tensor and ARFI images. All patients underwent parotid routine MRI and DTI on clinical 3.0-T MRI systems, routine ultrasound examination and ARFI on colour ultrasonic scanner before surgery. All patients signed the informed consent forms, and the local ethics committee approved the study.

### Image techniques

All examinations were performed on a Siemens Skyra 3.0-T MRI system and on ACUSON S2000 ultrasound scanners (Siemens Medical Solutions, Erlangen, Germany). DTI was performed using an eight-channel circular receiver head and neck coil. The parameters of the echoplanar sequence were the following: repetition time 3700 ms, echo time 95 ms, field of view 230 $\times$ 230 mm, section thickness of 4 mm with an intersection gap of 0 mm, $b$-values of 0 and 800 mm$^2$ s$^{-1}$, 20 orthogonal directions and acquisition time 4 min and 39 s.

ARFI imaging was performed by using a linear-array transducer 9L4 with a frequency of 7–12 MHz. Two-dimensional and Doppler images of lesions were observed multidimensionally. The transducer was gently put on the surface of parotid masses vertically, and the imaging mode was shifted to ARFI imaging by selecting the maximum cross-section of masses when images were clear. Then, regions of interest were selected in the solid of masses to avoid calcification, areas of sac and liquid dark regions. SWVs were recorded for each tumour.

*Image interpretation*
The workstation Siemens Syngo® Via 101532 (Siemens Healthcare, Erlangen Germany) was used to generate parametrical maps of ADC and FA after DTI. A standardized region-of-interest size of 40–50 mm$^2$ was drawn in the solid part of the parotid tumour and the mean values of ADC and FA were measured. The images were evaluated by two experienced radiologists by using the double-blind method. The acquisition and evaluation of all ARFI images were performed by two experienced doctors (15 and 20 years' experience in head and neck radiology).

*Statistical analysis*
All statistical analyses were performed with the statistical package for medical statistics (MedCalc® v. 15.6 for Windows; MedCalc, Ostend, Belgium). All the values of ADC, FA and SWV were presented as mean ± standard deviation ($\bar{x} \pm s$). For comparison of ADC, FA and SWV values between benign and malignant tumours, and between pleomorphic adenomas and adenolymphomas, independent samples Wilcoxon–Mann–Whitney test was conducted after Kolmogorov–Smirnov test for normal distribution. ANOVA was used for testing data homogeneity. With histopathological diagnosis as the gold standard and the maximum sum of the sensitivity and specificity, the cut-off values of ADC, FA and SWV for differentiating malignant from benign tumours and pleomorphic adenomas from adenolymphomas were obtained with receiver-operating characteristic (ROC) curve analysis; the sensitivity and specificity were also obtained with ROC analysis. For combination analysis, parallel test was performed to obtain the cut-off values of ADC, FA and SWV (combination = 0 or 1); then, ROC analysis was followed to attain the sensitivity, specificity, are under the ROC curve (AUC) and Youden index (*J*). $p < 0.05$ was considered to have a statistically significant difference.

**Results**

The sample of 51 parotid tumours consisted of 35 benign and 16 malignant tumours. In the 35 benign tumours, there were 16 pleomorphic adenomas, 15 adenolymphomas, 2 basal cell adenomas and 1 multiple nodular acidophil adenoma and 1 myoepithelioma. The 16 malignant tumours consisted of 5 mucoepidermoid carcinomas, 3 acinic cell carcinomas, 3 salivary duct carcinomas, 2 basal cell carcinomas, 1 adenoid cystic carcinoma, 1 adenocarcinoma and 1 carcinoma ex pleomorphic adenoma.

*Values of apparent diffusion coefficient, fractional anisotropy or shear-wave velocity are different between benign and malignant tumours*
Previous studies indicated that there was a significant difference in the ADC values between benign and malignant parotid tumours. ADC values could effectively predict the histological changes of salivary gland masses.[28,29] However, the use of SWV in the differential diagnosis of parotid tumours was controversial.[25,26] In order to further validate the previous reports and determine whether FA could be used to differentially diagnose malignant from benign parotid tumours, the values of ADC, FA and SWV were compared between benign and malignant tumours. ADC values were larger in benign tumours than in malignant tumours ($p = 0.0322$) (Table 1). SWV values were significantly greater in malignant tumours than in benign tumours ($p < 0.0001$) (Table 1), whereas FA values were significantly lower in benign tumours than in malignant tumours ($p = 0.0108$) (Table 1). Differences in these three values between benign and malignant tumours are also demonstrated in Figures 1 and 2.

*Values of apparent diffusion coefficient, fractional anisotropy and shear-wave velocity are different between pleomorphic adenoma and adenolymphoma*
There were reports showing that pleomorphic adenoma had the highest ADC values among all the benign tumours.[28,30] Adenolymphomas that are composed of lymphatic components surrounded by a capsule have lower SWV values.[26] To further validate the utility of ADC, FA and SWV in the differential diagnosis of pleomorphic adenoma from adenolymphoma, their values of ADC, FA and SWV were compared. In agreement with the above reports, values of ADC and SWV were significantly higher in pleomorphic adenoma than in adenolymphoma, whereas FA values were significantly lower in pleomorphic adenoma than in adenolymphoma ($p = 0.0012$ for ADC, $p < 0.0001$ for FA and $p = 0.0002$ for SWV) (Table 1).

*The cut-off, sensitivity and specificity values of apparent diffusion coefficient, fractional anisotropy and shear-wave velocity for the differential diagnosis of parotid tumours*
To obtain the cut-off values of the three parameters for the differential diagnosis of benign from malignant tumours, and pleomorphic adenoma from adenolymphoma, ROC analysis was performed; at the same time, the sensitivity and specificity were calculated. The cut-off points of ADC, FA and SWV were 1.02, 0.24 and 2.76 for the differential diagnosis of benign from malignant tumours, and they were 0.98, 0.19 and 2.03 for the differential diagnosis of pleomorphic adenoma from adenolymphoma (Tables 2 and 3 and Figure 3). The specificity and sensitivity for distinguishing benign and malignant tumours were 87.50% and 45.71% for ADC, 62.50% and 82.86% for FA and 68.75% and 97.14% for SWV (Table 2 and Figure 3). The specificity and sensitivity for differentiating pleomorphic adenomas from adenolymphomas were 80.00% and 81.25% for ADC, 93.33% and 93.75% for FA and 86.67% and 87.50% for SWV (Table 3 and Figure 4).

**Table 1** Comparison of apparent diffusion coefficient (ADC), fractional anisotropy (FA) and shear-wave velocity (SWV) values between malignant and benign tumours and between pleomorphic adenoma and adenolymphoma

| Pathological diagnosis | ADC ($10^{-3}$ $mm^2$ $s^{-1}$) | FA | SWV ($m\,s^{-1}$) | n |
|---|---|---|---|---|
| Malignant tumour | $0.82 \pm 0.22$ | $0.25 \pm 0.07$ | $2.94 \pm 0.39$ | 16 |
| Benign tumour | $1.04 \pm 0.37^a$ | $0.20 \pm 0.06^a$ | $2.09 \pm 0.52^b$ | 35 |
| Pleomorphic adenoma | $1.13 \pm 0.24$ | $0.16 \pm 0.03$ | $2.43 \pm 0.25$ | 16 |
| Adenolymphoma | $0.80 \pm 0.24^c$ | $0.24 \pm 0.03^d$ | $1.72 \pm 0.55^d$ | 15 |

Wilcoxon–Mann–Whitney test was used for statistical analysis.
[a] $p < 0.05$, compared with malignancy.
[b] $p < 0.0001$, compared with malignancy.
[c] $p < 0.01$, compared with pleomorphic adenoma.
[d] $p < 0.001$, compared with pleomorphic adenoma.

*Combination of the three parameters for the differential diagnosis of benign from malignant tumours*

To test whether the combination analysis of the three parameters is better than each alone in distinguishing benign from malignant tumours, parallel test was used for the cut-off values of ADC, FA and SWV. Variables including the sensitivity, specificity, AUC and Youden index (*J*) were obtained by ROC analysis (Table 2 and Figure 3). Combination of the three parameters is superior than ADC and FA alone for the differential diagnosis of benign from malignant tumours ($p = 0.0003$ and $p = 0.0043$).

## Discussion

DTI and ARFI imaging were valuable methods for the quantitative measurement of tissue histological properties. In the present study, they have proved to have merits for the differential diagnosis of parotid tumours. Compared with previous reports that evaluated DTI and ARFI imaging in parotid tumours, two prominent findings were revealed in our study: (1) in addition to ADC and SWV, FA was another valuable parameter for the differential diagnosis of benign from malignant tumours, and also for pleomorphic adenoma from
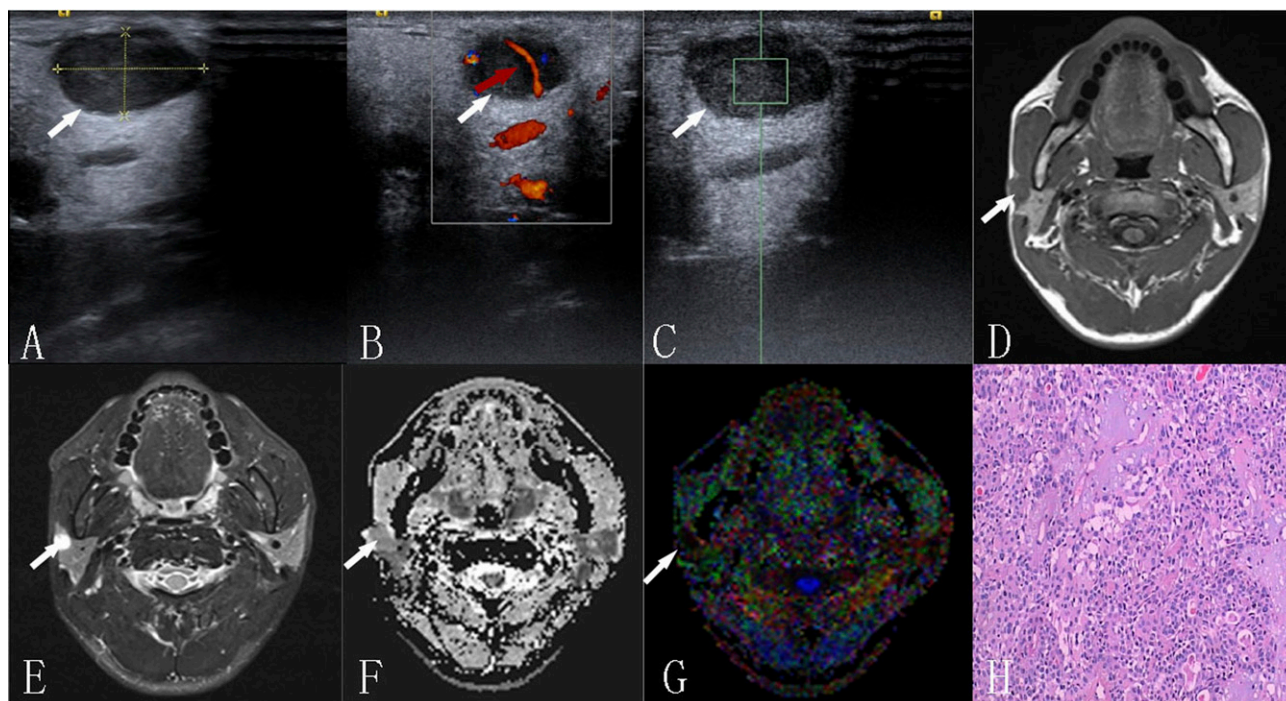


**Figure 1** A 32-year-old male with pleomorphic adenoma: (a) ultrasound—tumour is in the superficial lobe with well-defined borders and is showing hypoechogenicity; (b) colour Doppler flow imaging—curvilinear form vessels (arrow) are present inside the tumour; (c) the shear-wave velocity value within the region of interest is $2.32\,m\,s^{-1}$ with acoustic enhancement in high-resolution ultrasound; (d) the traverse $T_1$ weighted image is showing a well-defined isointense muscle mass; (e) the short time inversion-recovery $T_2$ weighted image is showing the homogeneous hyperintense mass; (f, g) apparent diffusion coefficient (ADC) and colour fractional anisotropy (FA) maps—tumour with an ADC value $1.43 \times 10^{-3}\,mm^2\,s^{-1}$ and an FA value of 0.17, respectively; and (h) haematoxylin–eosin staining ($\times100$).
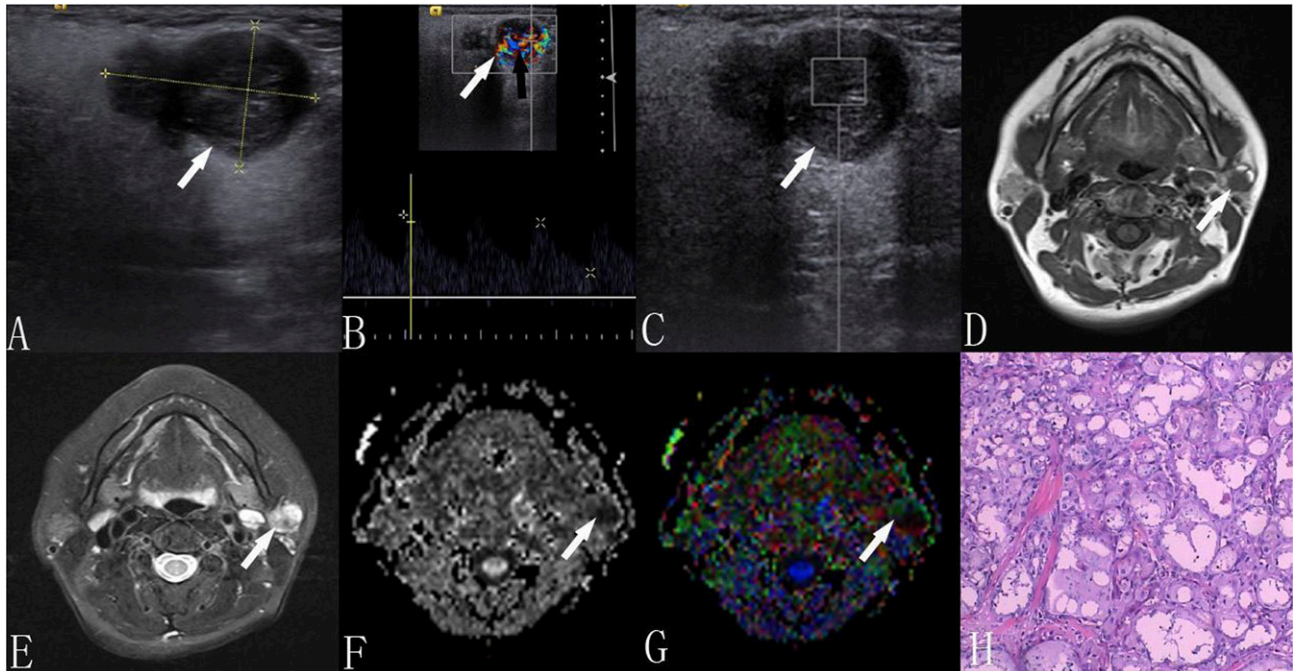
**Figure 2** A 56-year-old female with acnic cell carcinoma: (a) ultrasound—a hypoechoic mass with ill-defined borders having heterogeneity and a lobulated shape is present; (b) colour Doppler flow imaging is showing several vessels inside the tumour (black arrow); (c) the shear-wave velocity value within the user-defined region of interest is 2.43 m s$^{-1}$; (d) the traverse $T_1$ weighted image is showing an ill-defined high–low mixed mass; (e) the short time inversion-recovery $T_2$ weighted image is showing a heterogeneous hyperintense mass, in which the hypointense signal lies; (f, g) apparent diffusion coefficient (ADC) and colour fractional anisotropy (FA) maps—tumour with an ADC value of $0.69 \times 10^{-3}$ mm$^2$ s$^{-1}$ and an FA value of 0.29; and (h) haematoxylin–eosin staining ($\times$100).

adenolymphoma; (2) combination analysis of ADC, FA and SWV was superior than each alone for the differential diagnosis of malignant and benign tumours, and the sensitivity, specificity, AUC and Youden index ($J$) were increased.

ADC values could be affected by changes in the water molecule diffusion rate in the extracellular space. It was reported that ADC values could effectively distinguish the histological changes of salivary gland masses.[29] Irfan et al found that there was a significant difference in the ADC values between benign and malignant tumours, and between pleomorphic adenoma and adenolymphoma parotid tumours.[28] Similar results were revealed in our study. In contrast to Irfan et al,[28] we used 3.0-T high-field MR equipment and calculated ADC values with $b$ values of 0 and 800 s mm$^{-2}$. DTI in

3.0-T MRI has a higher signal-to-noise ratio and better image quality compared with 1.5-T MRI. ADC values were significant lower in malignant tumours than in benign tumours, which indicated a negative correlation between ADC value and cell density. However, the specificity and Youden index of ADC for distinguishing benign from malignant tumours were only 45.71% and 0.3321; this may have resulted from the similar ADC values between adenolymphomas and malignant tumours, because mucous cystic components and the capsule surrounding the tumour found in malignant tumours were also present in adenolymphomas tumours.[28]

In addition to ADC, values of FA, another parameter of DTI, were measured in our study. FA is an indicator for evaluating anisotropic sensitivity, and the FA value

**Table 2** Variables of receiver-operating characteristic (ROC) analysis for the three parameters analyzed either alone or in combination for the differential diagnosis of benign and malignant tumours

| Variables | ADC | FA | SWV | Combination |
|---|---|---|---|---|
| AUC | 0.69 | 0.76 | 0.91 | 0.92 |
| Cut-off point | 1.02 ($10^{-3}$ mm$^2$ s$^{-1}$) | 0.24 | 2.76 (m s$^{-1}$) | 0 |
| Sensitivity (with 95% CI) | 87.50 | 62.50 | 68.75 | 87.50 |
| Specificity % (with 95% CI) | 45.71 | 82.86 | 97.14 | 97.14 |
| $p$-value ($Z$-test) | 0.01 | 0.002 | <0.0001 | <0.0001 |
| Youden index ($J$) | 0.33 | 0.45 | 0.66 | 0.85 |

ADC, apparent diffusion coefficient; AUC, area under the ROC curve; CI, confidence interval; FA, fractional anisotropy; SWV, shear-wave velocity.
For combination analysis, parallel test was conducted first to obtain the combination, followed by ROC analyses to acquire all variables.

**Table 3** Variables of receiver-operating characteristic (ROC) analysis for three parameters each alone for the differential diagnosis of pleomorphic adenoma and adenolymphoma

| Variables | ADC | FA | SWV |
|---|---|---|---|
| AUC | 0.84 | 0.98 | 0.89 |
| Cut-off point | 0.98 ($10^{-3}\,mm^2\,s^{-1}$) | 0.19 | 2.03 ($m\,s^{-1}$) |
| Sensitivity (with 95% CI) | 80.00 | 93.33 | 86.67 |
| Specificity % (with 95% CI) | 81.25 | 93.75 | 87.5 |
| *p*-value (*Z* test) | <0.0001 | <0.0001 | <0.0001 |
| Youden index (*J*) | 0.61 | 0.87 | 0.74 |

ADC, apparent diffusion coefficient; AUC, area under the ROC curve; CI, confidence interval; FA, fractional anisotropy; SWV, shear-wave velocity.
All the variables were obtained with ROC analysis.

range is 0–1. FA values equal 0 for the isotropic condition, in which diffusion is equal in all directions, and FA values approach a value of 1 for extreme directional inequality. To our knowledge, no studies with regard to FA application in the differential diagnosis of parotid tumours have been reported. It was reported that the positive correlation of the FA value with tumour cellularity, that is higher FA, was associated with higher tumour cellularity.[18,22–24] In agreement with previous studies in other organs, our results showed that malignant parotid tumours had higher FA values than benign tumours. In our study, there was a significant difference in the FA values not only between benign and malignant tumours but also between pleomorphic adenomas and adenolymphomas. The decreased diffusivity and increased anisotropy in parotid malignant tumours may be explained by cell density increase, which might have caused water molecules to diffuse with a higher degree

of directionality, in contrast to benign tumours.[24] Our results also showed that FA had higher specificity than ADC in distinguishing benign and malignant tumours, and in distinguishing pleomorphic adenoma and adenolymphoma. Moreover, compared with ADC, FA exhibited higher sensitivity and specificity for distinguishing pleomorphic adenoma and adenolymphoma. Therefore, FA could be used as another effective parameter for the differential diagnosis of parotid tumours.

ARFI imaging-based elastography was designed to characterize the mechanical properties of tissues by using a short-duration acoustic radiation force to generate a shear wave from the excitation region of the tissue. The shear wave can be easily tracked and the propagation distance per second, *i.e.* SWV, can be calculated by a quantitative implementation named virtual touch imaging quantification.[25,31,32] The higher the elasticity and hardness of the tissue, the farther the shear-wave propagation will be, and the greater the SWV value will
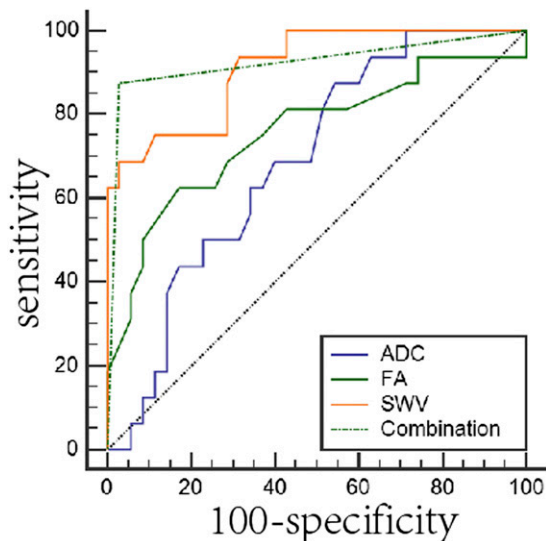


**Figure 3** The receiver-operating characteristic (ROC) analysis of three parameters each alone and in combination for the diagnosis of benign and malignant parotid tumours: for combination analysis, parallel test was performed to acquire the new variation combination, followed by ROC analysis. The area under the ROC curve (AUC) below the black dotted line is <0.5. The sensitivity, specificity, AUC of the combination is bigger than those of apparent diffusion coefficient (ADC), fractional anisotropy (FA) and shear-wave velocity (SWV) each alone.
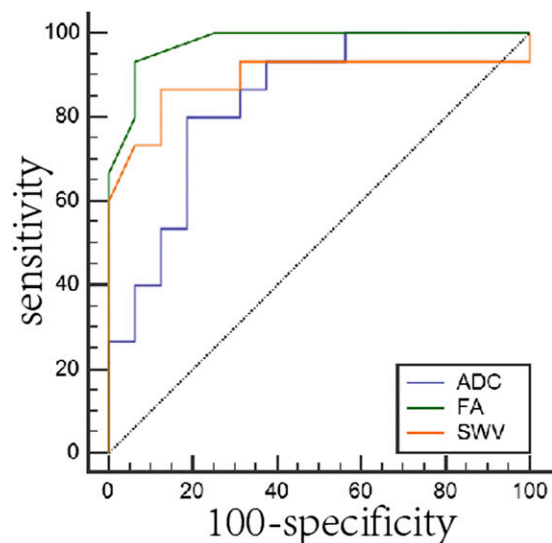


**Figure 4** The receiver-operating characteristic (ROC) analysis of three parameters for the diagnosis of pleomorphic adenoma and adenolymphomas: the area under the ROC curve (AUC) below the black dotted line is <0.5. Fractional anisotropy (FA) had the largest AUC, sensitivity and specificity, while apparent diffusion coefficient (ADC) had the smallest AUC. SWV, shear-wave velocity.

be.[25] Stiffness and elasticity of lesions could be changed with alterations of cancer cellular density, components of the tissue and blood vessels. ARFI imaging was developed in 2009.[33] Similar to FA, values of SWV were proved to be positively correlated with cell density.[18,25] In agreement with this idea, our results showed that malignant tumours had the highest SWV values. A significant difference of SWV values was revealed between pleomorphic adenoma and adenolymphoma, but there was no significant difference between benign and malignant tumours.[26] In contrast, another study from Matsuzuka et al[25] reported a significant difference in the SWV values between benign and malignant tumours. Our study indicated a significance difference in the mean SWV values not only between benign and malignant tumours, but also between pleomorphic adenoma and adenolymphoma. Different findings from our study and other studies may be attributed to the fact that measurements of SWV in malignant tumours were performed with virtual touch imaging quantification in our study, and they could not be obtained beyond the range with virtual touch quantification in the previous study.[25]

In addition to the comparison of FA, ADC and SWV values each alone, we also did the combination analysis for the three parameters with parallel test and ROC analysis. Our results showed that combination analysis was superior to each alone for distinguishing benign from malignant tumours. For ROC analysis, AUC is a measure of the "overall diagnostic performance", because it averages all possible diagnostic thresholds.[34,35] The Youden index (*J*) is usually used to

evaluate the clinical diagnostic ability of a test[36] and is an optimal trade-off relative to sensitivity and specificity, but with the same weight for sensitivity and specificity. In our study, the sensitivity, specificity, AUC and Youden index (*J*) of the combination analysis were improved relative to the three parameters each alone for distinguishing benign and malignant parotid tumours, which suggested the superiority of combination analysis. ROC analysis showed that there was a statistical difference between AUCs of combination analysis and both ADC and FA ($p = 0.0003$ and $p = 0.0043$). This suggests that the diagnostic value of the combination of the three parameters is the best for distinguishing benign from malignant parotid tumours.

There were several limitations in our study. The patients had a large age span; the total amount of patients was relatively small; and the number of cases in each subgroup was low. These limitations may attribute to the differences between some of our conclusions and those of other reports and also prevented us from the evaluation of combination analysis for the differential diagnosis of pleomorphic adenoma and adenolymphoma. Therefore, these results have to be considered as preliminary and need further investigations for confirmation.

In conclusion, parameters of DTI and ARFI might reflect the microstructure of parotid tumours and therefore could provide quantitative information for the tumour. Combination of DTI with ARFI imaging had obvious advantage for diagnosing and differentially diagnosing parotid tumours than each alone.

## References

1. Pinkston JA, Cole P. Incidence rates of salivary gland tumors: results from a population-based study. *Otolaryngol Head Neck Surg* 1999; **120**: 834–40. doi: http://dx.doi.org/10.1016/S0194-5998(99)70323-2

2. Seifert G. *Histoligical typing of salivary gland tumors*. 2nd edn. Berlin, Germany: Springer-Verlag; 1991. pp. 24–54.

3. Donovan DT, Conley JJ. Capsular significance in parotid tumor surgery: reality and myths of lateral lobectomy. *Laryngoscope* 1984; **94**: 324–9. doi: http://dx.doi.org/10.1288/00005537-198403000-00006

4. Woods JE, Chong GC, Beahrs OH. Experience with 1,360 primary parotid tumors. *Am J Surg* 1975; **130**: 460–2. doi: http://dx.doi.org/10.1016/0002-9610(75)90484-5

5. Heller KS, Attie JN. Treatment of Warthin's tumor by enucleation. *Am J Surg* 1988; **156**: 294–6. doi: http://dx.doi.org/10.1016/S0002-9610(88)80295-2

6. Witt RL. The significance of the margin in parotid surgery for pleomorphic adenoma. *Laryngoscope* 2002; **112**: 2141–54. doi: http://dx.doi.org/10.1097/00005537-200212000-00004

7. Myssiorek D, Ruah CB, Hybels RL. Recurrent pleomorphic adenomas of the parotid gland. *Head Neck* 1990; **12**: 332–6. doi: http://dx.doi.org/10.1002/hed.2880120410

8. Brieger J, Duesterhoeft A, Brochhausen C, Gosepath JAN, Kirkpatrick CJ, Mann WJ. Recurrence of pleomorphic adenoma of the parotid gland—predictive value of cadherin-11 and fascin. *APMIS* 2008; **116**: 1050–7. doi: http://dx.doi.org/10.1111/j.1600-0463.2008.01088.x

9. Wennmo C, Spandow O, Emgard P, Krouthen B. Pleomorphic adenomas of the parotid gland: superficial parotidectomy or limited excision? *J Laryngol Otol* 1988; **102**: 603–5. doi: http://dx.doi.org/10.1017/S0022215100105845

10. Henriksson G, Westrin KM, Carlsöö B, Silfverswärd C. Recurrent primary pleomorphic adenomas of salivary gland origin: intrasurgical rupture, histopathologic features, and pseudopodia. *Cancer* 1998; **82**: 617–20. doi: http://dx.doi.org/10.1002/(SICI)1097-0142(19980215)82:4<617::AID-CNCR1>3.0.CO;2-I

11. Bialek EJ, Jakubowski W, Zajkowski P, Szopinski KT, Osmolski A. US of the major salivary glands: anatomy and spatial relationships, pathologic conditions, and pitfalls. *Radiographics* 2006; **26**: 745–63. doi: http://dx.doi.org/10.1148/rg.263055024

12. Habermann CR, Arndt C, Graessner J. Diffusion-weighted echoplanar MR imaging of primary parotid gland tumors: is a prediction of different histologic subtypes possible? *Am J Neuroradiol* 2009; **30**: 591–6. doi: http://dx.doi.org/10.3174/ajnr.A1412

13. Bozzato A, Zenk J, Greess H, Hornung J, Gottwald F, Rabe C. Potential of ultrasound diagnosis for parotid tumors: analysis of qualitative and quantitative parameters. *Otolaryngol Head Neck Surg* 2007; **137**: 642–6. doi: http://dx.doi.org/10.1016/j.otohns.2007.05.062

14. Bhatia KS, Rasalkar DD, Lee YP. Evaluation of real-time qualitative sonoelastography of focal lesions in the parotid and submandibular glands: applications and limitations. *Eur Radiol* 2010; **20**: 1958–64. doi: http://dx.doi.org/10.1007/s00330-010-1756-0

15. Merboldt KD, Hänicke W, Frahm J. Diffusion imaging using stimulated echoes. *Magn Reson Med* 1991; **19**: 233–9. doi: http://dx.doi.org/10.1002/mrm.1910190208

16. Nomura Y, Sakuma H, Takeda K, Tagami T, Okuda Y, Nakagawa T. Diffusional anisotropy of the human brain assessed with diffusion-weighted MR: relation with normal brain development and aging. *Am J Neuroradiol* 1994; **15**: 231–8.

17. Pierpaoli C, Jezzard P, Basser PJ, Barnett A, Di Chiro G. Diffusion tensor MR imaging of the human brain. *Radiology* 1996; **201**: 637–48. doi: http://dx.doi.org/10.1148/radiology.201.3.8939209

18. Kinoshita M, Hashimoto N, Goto T, Kagawa N, Kishima H, Izumoto S, et al. Fractional anisotropy and tumor cell density of the tumor core show positive correlation in diffusion tensor magnetic resonance imaging of malignant brain tumors. *Neuroimage* 2008; **43**: 29–35. doi: http://dx.doi.org/10.1016/j.neuroimage.2008.06.041

19. Sugita R, Ito K, Fujita N, Takahashi S. Diffusion-weighted MRI in abdominal oncology: clinical applications. *World J Gastroenterol* 2010; **16**: 832–6.

20. Filippi CG, Edgar MA, Uluğ AM, Prowda JC, Heier LA, Zimmerman RD. Appearance of meningiomas on diffusion-weighted images: correlating diffusion constants with histopathologic findings. *Am J Neuroradiol* 2001; **22**: 65–72.

21. Taouli B, Martin AJ, Qayyum A. Parallel imaging and diffusion tensor imaging for diffusion-weighted MRI of the liver: preliminary experience in healthy volunteers. *AJR Am J Roentgenol* 2004; **183**: 677–80. doi: http://dx.doi.org/10.2214/ajr.183.3.1830677

22. Gürses B, Tasdelen N, Yencilek F. Diagnostic utility of DTI in prostate cancer. *Eur J Radiol* 2011; **79**: 172–6. doi: http://dx.doi.org/10.1016/j.ejrad.2010.01.009

23. Erturk SM, Ichikawa T, Kaya E, Yapici O, Ozel A, Mahmutoglu AS, et al. Diffusion tensor imaging of cysts, hemangiomas, and metastases of the liver. *Acta Radiol* 2013; **55**: 654–60. doi: http://dx.doi.org/10.1177/0284185113504916

24. Tsougos I, Svolos P, Kousi E, Athanassiou E, Theodorou K, Arvanitis D, et al. The contribution of diffusion tensor imaging and magnetic resonance spectroscopy for the differentiation of breast lesions at 3T. *Acta Radiol* 2014; **55**: 14–23. doi: http://dx.doi.org/10.1177/0284185113492152

25. Matsuzuka T, Suzuki M, Saijo S. Stiffness of salivary gland and tumor measured by new ultrasonic techniques: virtual touch quantification and IQ. *Auris Nasus Larynx* 2015; **42**: 128–33. doi: http://dx.doi.org/10.1016/j.anl.2014.08.021

26. Mansour N, Stock KF, Chaker A, Bas M, Knopf A. Evaluation of parotid gland lesions with standard ultrasound, color duplex sonography, sonoelastography, and acoustic radiation force impulse imaging—a pilot study. *Ultraschall Med* 2012; **33**: 283–8. doi: http://dx.doi.org/10.1055/s-0031-1299130

27. Eveson JW, Auclair P, Gnepp DR. Tumours of the salivary glands. In: Barnes L, Eveson JW, Reichart P, eds. *World Health Organisation classification of tumours: pathology and genetics of head and neck tumours.* Lyon, France: IARC Press; 2005. pp. 212–15.

28. Celebi I, Mahmutoglu AS, Ucgul A, Ulusay SM, Basak T, Basak M. Quantitative diffusion-weighted magnetic resonance imaging in the evaluation of parotid gland masses: a study with histopathological correlation. *Clin Imaging* 2013; **37**: 232–8. doi: http://dx.doi.org/10.1016/j.clinimag.2012.04.025

29. Eida S, Sumi M, Sakihama N, Takahashi H, Nakamura T. Apparent diffusion coefficient mapping of salivary gland tumors: prediction of the benignancy and malignancy. *AJNR Am J Neuroradiol* 2007; **28**: 116–21.

30. Motoori K, Yamamoto S, Ueda T. Inter- and intratumoral variability in magnetic resonance imaging of pleomorphic adenoma: an attempt to interpret the variable magnetic resonance findings. *J Comput Assist Tomogr* 2004; **28**: 233–46. doi: http://dx.doi.org/10.1097/00004728-200403000-00014

31. Yeshua H, Oren R. Non invasive assessment of liver fibrosis. *Ann Transplant* 2008; **13**: 5–11.

32. D'Onofrio M, Crosara S, De Robertis R. Acoustic radiation force impulse of the liver. *World J Gastroenterol* 2013; **19**: 4841–9.

33. Cassinotto C, Lapuyade B, Mouries A. Non-invasive assessment of liver fibrosis with impulse elastography: comparison of supersonic shear imaging with ARFI and FibroScan®. *J Hepatol* 2014; **61**: 550–7. doi: http://dx.doi.org/10.1016/j.jhep.2014.04.044

34. Hanley A, Mcneil J. The meaning and use of the area under a receiver operating characteristic (ROC) curve. *Radiology* 1982; **143**: 29–36. doi: http://dx.doi.org/10.1148/radiology.143.1.7063747

35. Park SH, Goo JM, Jo CH. Receiver operating characteristic (ROC) curve: practical review for radiologists. *Korean J Radiol* 2004; **5**: 11–18. doi: http://dx.doi.org/10.3348/kjr.2004.5.1.11

36. Youden WJ. Index for rating diagnostic tests. *Cancer* 1950; **3**: 32–5. doi: http://dx.doi.org/10.1002/1097-0142(1950)3:1<32::AID-CNCR2820030106>3.0.CO;2-3